Misalignment characteristics of resonators formed by 90° cone and mirror

J. Y. Liou, C. J. Chen, and M. Y. Hwang

The stability condition of a resonator formed by a 90° cone and mirror has been derived using ray tracing techniques. The result showed that this type of resonator is relatively insensitive to mirror misalignment. From this basis, the mirror misalignment tolerance was studied experimentally. Output energy and transverse mode characteristics vs. misalignment were measured, and the results show that this type of resonator does possess certain advantages over the two-mirror resonator.

I. Introduction

A total internal reflector, suggested as a laser resonator in Ref. 1, has the advantage of no metallic or multilayer dielectric coating and hence reduced heating effect and threshold pumping power. However, the proposed frustrated total reflection coupling scheme is relatively inconvenient and difficult for performing such techniques as Q-switching and mode locking. Thus we consider the laser resonator formed by a 90° cone and mirror as shown in Fig. 1. This type of resonator has the advantage of minimizing the number of dissipative coatings, and it preserves the possibility of modulation within the resonator. Similar structures have been discussed before,[2–4] but to our knowledge there is little in the literature[5,6] discussing the stability condition in terms of ray tracing techniques, and few experimental results have been published. This paper is thus concerned with a discussion of the stability condition and the measurement of transverse mode characteristics of this particular resonator, emphasizing the misalignment effect that is one of the most important factors in field operation. We have called this the cone–mirror resonator.

The authors are with National Chiao Tung University, Hsinchu, Taiwan, China.

Received 26 January 1980.
0003-6935/80/152569-05$00.50/0.

II. Stability Conditions of Cone–Mirror Resonator

In the following analysis, the meridian ray transfer matrix for a nearly 90° cone reflector is derived first, then this matrix is used to determine the stability condition of the cone–mirror resonator.

A. Ray Transfer Matrix for Nearly 90° Cone Reflectors

Assume that we have a nearly 90° reflector as shown in Fig. 2 and that the incoming meridian paraxial ray hits upper surface F_1 first, then reflecting surfaces F_1, F_2. Assume further that the incoming rays are

$$y = -(x - a)\tan\gamma, \tag{1}$$

$$y = (x - a)\tan\xi, \tag{2}$$

$$y = y_0 + x\tan\mu_0, \tag{3}$$

where the various parameters are defined in Fig. 2, and where $\gamma = (\pi/4) + \delta$, $\xi\ (\pi/4) + \phi$, with the assumption that $|\delta| \ll 1$, $|\phi| \ll 1$ and $|\mu_0| \ll 1$.

The outgoing ray, which is the incoming ray after reflection from surfaces F_1 and F_2, is characterized by its slope μ_0' and height y_0' at plane $X = 0$ as shown in Fig. 2. These two quantities can be derived with geometric optics. Using the approximation

$$\tan(\pi/4 + \delta) \simeq 1 + 2\delta, \quad \tan(\pi/4 + \phi) \simeq 1 + 2\phi, \quad \tan\mu_0 \simeq \mu_0,$$

we find that

$$\mu_0' \simeq \mu_0 + 2(\phi + \delta), \tag{4}$$

$$y_0' \simeq -y_0 - 2a\mu_0 - 2a(\delta + \phi). \tag{5}$$

If we define rays 1 and 2 (upgoing) in Fig. 3 as having positive slopes, rays 3 and 4 (downgoing) have negative slopes. We can then combine Eqs. (4) and (5) and write the ray transfer matrix as Eq. (6) for those paraxial rays

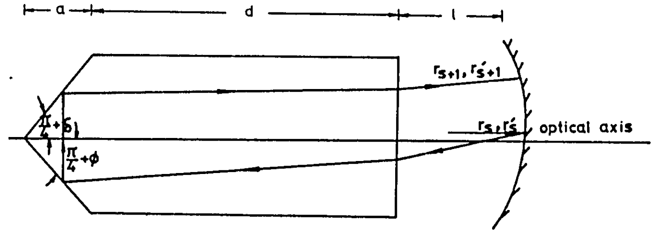

Fig. 1. Schematic diagram used to derive the stability condition of a cone–mirror resonator.

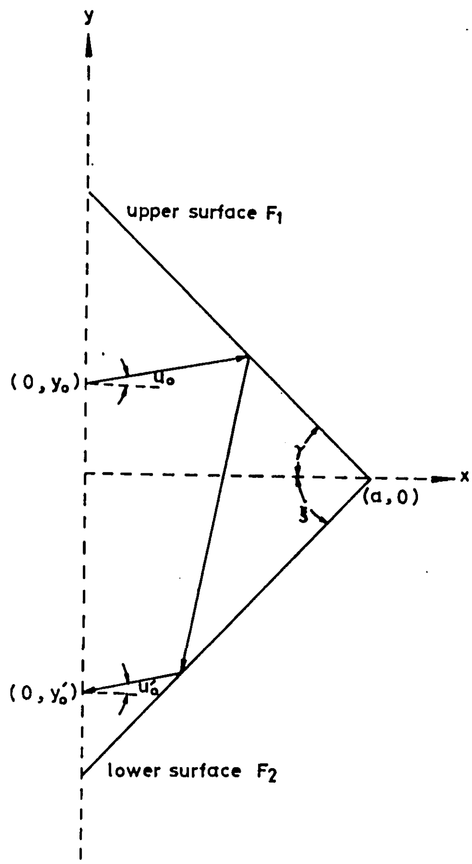

Fig. 2. Schematic diagram used to derive the ray transfer matrix for a nearly 90° cone reflector.

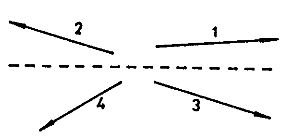

Fig. 3. Schematic diagram used to define the sign of the slope of the rays, where rays 1 and 2 are defined with positive slopes and rays 3 and 4 with negative slopes.

that hit the upper surface first:

$$\begin{bmatrix} r_0 \\ r_0' \end{bmatrix} = \begin{bmatrix} -1 & -2a \\ 0 & -1 \end{bmatrix} \begin{bmatrix} r_i \\ r_i' \end{bmatrix} - \begin{bmatrix} 2a(\delta + \phi) \\ 2(\delta + \phi) \end{bmatrix}, \tag{6}$$

where r_i = height of incoming ray at plane $X = 0$ (corresponding to y_0 in Fig. 2);
r_0 = height of outgoing ray at plane $X = 0$ (corresponding to y_0' in Fig. 2);
r_i' = slope of incoming ray (corresponding to $\tan \mu_0 \simeq \mu_0$ in Fig. 2); and
r_0' = slope of outgoing ray (corresponding to $-\tan\mu_0' \simeq -(\mu_0 + 2\delta + 2\phi)$; the minus sign is due to the choice of negative slope defined in Fig. 2.

With the same derivation procedure, we find that when a ray hits the lower surface (F_2 in Fig. 2) first, the ray transfer matrix will be

$$\begin{bmatrix} r_0 \\ r_0' \end{bmatrix} = \begin{bmatrix} -1 & -2a \\ 0 & -1 \end{bmatrix} \begin{bmatrix} r_i \\ r_i' \end{bmatrix} + \begin{bmatrix} 2a(\delta + \phi) \\ 2(\delta + \phi) \end{bmatrix}. \tag{7}$$

The difference of the sign of the constant term in Eqs. (6) and (7) can be understood by considering the fact that the height and slope of a ray are always inverted after reflection from a nearly 90° reflector when the sign of the slope is defined as in Fig. 2.

For clarity, the ray transfer matrices for different combinations of incoming paraxial rays and reflector surface are shown in Table I. For those rays that hit the upper surface (surface above the optical axis) first, the sign of the constant term [such as in Eq. (6)] is negative; for those rays that hit the lower surface (below the optical axis) first, the sign is positive.

B. Stability Condition

The structure of the resonator under consideration is of the form shown in Fig. 1, where the left is a solid-state laser rod (such as Nd:YAGs) with one end polished as a 90° cone and the other end polished to a flat surface. Total internal reflection occurs for paraxial rays because of the difference of the index of refraction between air and the laser rod. The mirror has a radius of curvature R. The quantities δ and ϕ are manufacturing tolerances or the slight tilt of the optical axis due to misalignment.

To study how δ and ϕ affect the stability of such a resonator, we write the matrices describing the propagation of paraxial rays shown in Fig. 1:

$$\begin{bmatrix} r_{s+1} \\ r_{s+1}' \end{bmatrix} = \begin{bmatrix} 1 & l \\ 0 & 1 \end{bmatrix} \begin{bmatrix} 1 & 0 \\ 0 & n \end{bmatrix} \begin{bmatrix} 1 & d \\ 0 & 1 \end{bmatrix} \left\{ \begin{bmatrix} -1 & -2a \\ 0 & -1 \end{bmatrix} \begin{bmatrix} 1 & d \\ 0 & 1 \end{bmatrix} \right.$$

$$\left. \times \begin{bmatrix} 1 & 0 \\ 0 & \frac{1}{n} \end{bmatrix} \begin{bmatrix} 1 & l \\ 0 & 1 \end{bmatrix} \begin{bmatrix} 1 & 0 \\ -\frac{2}{R} & 1 \end{bmatrix} \begin{bmatrix} r_s \\ r_s' \end{bmatrix} + \begin{bmatrix} 2a(\delta + \phi) \\ 2(\delta + \phi) \end{bmatrix} \right\}$$

$$= \begin{bmatrix} A & B \\ C & D \end{bmatrix} \begin{bmatrix} r_s \\ r_s' \end{bmatrix} + \begin{bmatrix} E \\ F \end{bmatrix},$$

Table I. Ray Transfer Matrices for Possible Combination of Nearly 90° Reflectors and Incoming Rays, $\gamma = \pi/4 + \delta$, $\xi = \pi/4 + \varphi$; $\delta \ll 1$, $\varphi \ll 1$

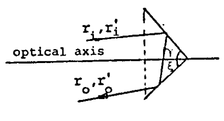	$\begin{bmatrix} r_o \\ r'_o \end{bmatrix} = \begin{bmatrix} -1 & -2a \\ 0 & -1 \end{bmatrix} \begin{bmatrix} r_i \\ r'_i \end{bmatrix} - \begin{bmatrix} 2a(\delta+\phi) \\ 2(\delta+\phi) \end{bmatrix}$
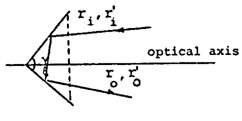	$\begin{bmatrix} r_o \\ r'_o \end{bmatrix} = \begin{bmatrix} -1 & -2a \\ 0 & -1 \end{bmatrix} \begin{bmatrix} r_i \\ r'_i \end{bmatrix} - \begin{bmatrix} 2a(\delta+\phi) \\ 2(\delta+\phi) \end{bmatrix}$
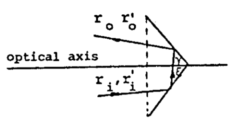	$\begin{bmatrix} r_o \\ r'_o \end{bmatrix} = \begin{bmatrix} -1 & -2a \\ 0 & -1 \end{bmatrix} \begin{bmatrix} r_i \\ r'_i \end{bmatrix} + \begin{bmatrix} 2a(\delta+\phi) \\ 2(\delta+\phi) \end{bmatrix}$
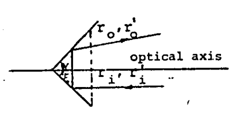	$\begin{bmatrix} r_o \\ r'_o \end{bmatrix} = \begin{bmatrix} -1 & -2a \\ 0 & -1 \end{bmatrix} \begin{bmatrix} r_i \\ r'_i \end{bmatrix} + \begin{bmatrix} 2a(\delta+\phi) \\ 2(\delta+\phi) \end{bmatrix}$

where n is the index of refraction of the laser rod and r_s, r'_s are height and slope of the paraxial ray before incident on the mirror surface. Also, we have

$$A = -1 + \frac{4}{R}\left(l + \frac{a+d}{n}\right),$$

$$B = -2\left(l + \frac{a+d}{n}\right),$$

$$C = 2/R,$$

$$D = -1,$$

$$E = 2(nl + a + d)(\delta + \phi),$$

$$F = 2n(\delta + \phi).$$

Following a similar mathematical manipulation to that used in Ref. 7, we obtain the difference equation

$$r_{s+2} - 2\left[1 - \frac{2}{R}\left(l + \frac{a+d}{n}\right)\right] r_{s+1} + r_s = 0.$$

The stability condition of this equation is given by

$$0 \le 1 - \frac{1}{R}\left(l + \frac{a+d}{n}\right) \le 1. \qquad (8)$$

One important result of Eq. (8) is that the stability condition of the cone–mirror resonator is independent of δ and ϕ. In other words, this type of resonator is insensitive to small aberrations. This is important in field operation where vibration can be serious because it usually causes mirror misalignment. Misalignment is also a problem in a high repetition rate laser because thermal stress will also induce mirror misalignment.

III. Experimental Results

In this experiment, the Nd:YAG laser rod (69 mm long, 5-mm diam, 1.2% Nd^{3+} concentration, with the same end configurations as shown in Fig. 1) was put into a gold-coated circular cavity and pumped by a pulsed xenon flashlamp. The typical discharging condition was 50 μF and 600 V. To avoid any heating effect, pulses were taken at 0.05 pulse/sec.

The output mirror is a plane mirror with reflectivity equal to 70%. This mirror is mounted in a mirror holder whose plane can be tilted by micrometers in both X and Y directions. Cavity length is 20 cm. Output energy was detected by a silicon P-I-N photodiode (with RG > 80, 1.06-μm filter in front of the detector) with 0.25-mm^2 active area, and it was mounted on a translation stage. Each data point in Figs. 5–7 is an average of five experimental results. The oscilloscope trace of Fig. 4 shows a sudden rise of output energy confirming that laser oscillation does occur in such a resonator.

A. Output Energy vs Mirror Misalignment

In field operation, vibration and thermally induced stress will cause mirror misalignment, and small misalignment will usually cause significant reduction of output energy in a two-mirror resonator.[8,9] In a cone–mirror resonator, the output energy is relatively insensitive to mirror misalignment because of the retroreflective properties of the 90° cone as discussed in Sec. II, where the stability condition of the cone–mirror resonator is independent of small misalignment. Figure 5 shows detected output energy vs mirror misalignment; the misalignment effect of a two-mirror resonator is plotted in the same figure. It is clear that the cone–mirror resonator is ~200 times more stable compared with a two-mirror resonator if the point where 10% reduction of the output energy is taken as the reference.

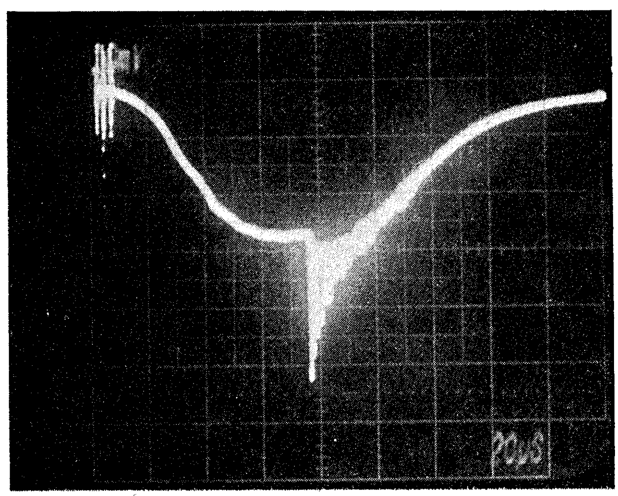

Fig. 4. Pulsed output of a Nd:YAG laser with a cone–mirror resonator.

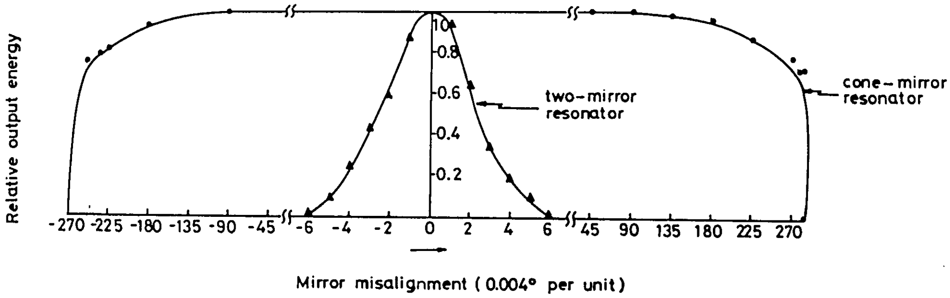

Fig. 5. Output energy vs absolute mirror misalignment for both cone–mirror and two-mirror resonators.

In a two-mirror system, the length of the laser rod is 65 mm, the totally reflective mirror has an $R = 10$-m radius of curvature, and the output mirror is that used in the cone–mirror resonator. (Cavity length is also 20 cm.) Pumping conditions are the same as those in a cone–mirror system.

B. Transverse Intensity Distribution

Figure 6 shows the near-field distribution of the laser beam when the mirror is well aligned. Here this means that the mirror is at the center position of Fig. 5. Ideal Gaussian distribution is plotted in the same figure for comparison; they are quite similar to each other.

In Fig. 7 the near-field distribution with a misaligned mirror is plotted in comparison with that of a well-aligned system. It is clear from this figure that the spatial distribution of the laser beam is almost unaffected by mirror misalignment. This is also due to retroreflective properties. During these measurements, no iris was used. We found that the cone–mirror resonator tends to oscillate in the lowest order mode even in the case of a misaligned mirror.

C. Beam Divergence

The spatial distribution of the laser beam was measured at two different points with 50-cm separation and the beam diameter determined at the $1/e^2$ intensity points relative to the maximum. It was found that the laser beam has a divergence angle of ~2.5°, which is relatively large compared with that of the two-mirror resonator.[9] We tend to conclude that this large divergence angle is a characteristic of the cone–mirror resonator and is not due to the near-threshold pumping power because two mirrors with different reflectivities (one with 40%, the other 70%) were used in this measurement, and similar results were obtained.

To explain this divergence phenomenon and the transverse mode intensity distribution, a diffraction theory approach to this problem is required. This is currently under study and will be discussed in a later paper.

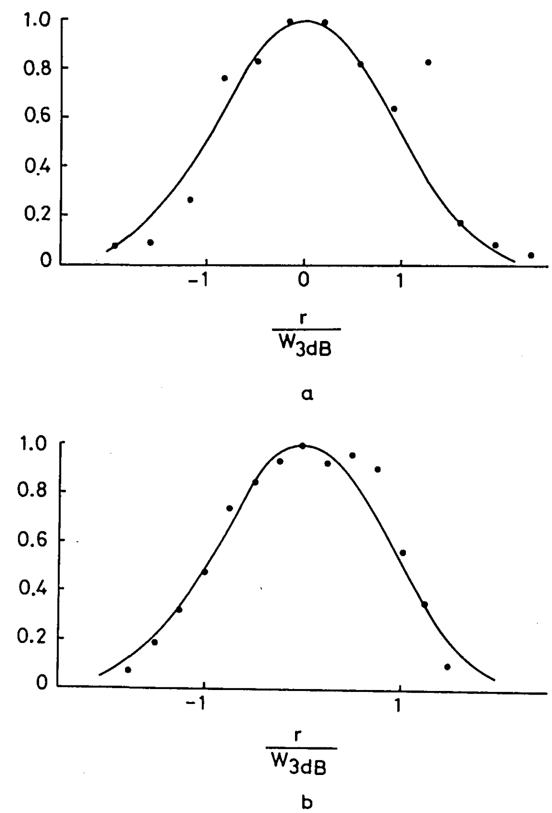

Fig. 6. Comparison of intensity distribution with an ideal Gaussian distribution of the same width at the half-power point: (a) near-field distribution, (b) far-field distribution.

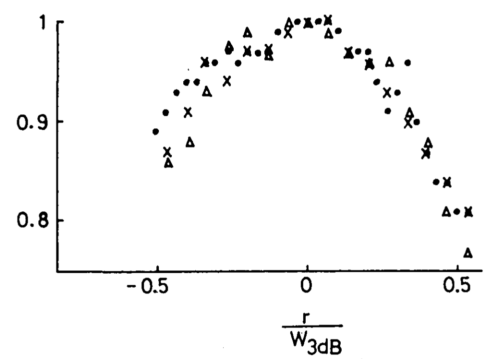

Fig. 7. Comparison of intensity distribution for well-aligned and misaligned mirrors, where ● represent well-aligned data and △ (×) represent the mirror tilted by +(−) 0.36°.

IV. Conclusion

From both theory and experimental results, the cone–mirror resonator appears to have advantages over a two-mirror resonator as far as misalignment is concerned; this is important in field operation. Although a relatively large beam divergence was observed, this will not become a major defect in laser application because it can be easily corrected by external optics, as is also necessary in a laser beam from a two-mirror resonator.

Although the results have been directly concerned with the performance of a Nd:YAG laser, the conclusion should be applicable to other lasers. In gas and liquid lasers, the total internal 90° cone reflector can be replaced by a 90° cone with a mirror surface (such as polishing a copper rod to obtain this particular shape); similar results should be expected.

References

1. L. Bernstein, W. Kahn, and G. Schulman, Proc. IRE **50**, 1833 (1965).
2. E. R. Peck, J. Opt. Soc. Am. **52**, 253 (1962).
3. L. Ronchi, Appl. Opt. **12**, 93 (1973).
4. F. Pasqualetti and L. Ronchi, J. Opt. Soc. Am. **64**, 289 (1974).
5. G. Soncini and O. Svelto, Appl. Phys. Lett. **11**, 261 (1967).
6. G. J. Linford and L. W. Hill, Appl. Opt. **13**, 1387 (1974).
7. A. Yariv, *Introduction to Optical Electronics* (Holt, Rinehart, and Winston, New York, 1971), Chap. 2.
8. R. J. Freiberg and A. S. Halsted, Appl. Opt. **8**, 355 (1969).
9. W. Koechner, *Solid-State Laser Engineering* (Springer, New York, 1976), p. 194.

Meetings Calendar *continued from page 2559*

1980

September

10–12 Optical Group Biennial Conf., U. Manchester Inst. Sci. and Tech. *P. M. J. H. Wormell, Blackett Lab., Imperial Coll., Prince Consort Rd., London SW7 2BZ, England*

15–19 New Methods in Microscopy (Advanced Microscopy) course, Chicago *N. Daerr, McCrone Res. Inst., 2508 S. Michigan Ave., Chicago, Ill. 60616*

16–18 Fiber Optics and Communications Expo., 3rd Int., San Francisco *M. A. Bryant, Information Gatekeepers, 167 Corey Rd., Suite 111, Brookline, Mass. 02146*

16–18 6th European Conf. On Optical Communication, U. York, U.K. *OSA, 1816 Jefferson Pl. N.W., Wash., D.C. 20036*

16–19 European Signal Processing Conf., Lausanne *M. Kunt, Lab. de traitement des signaux, 16, ch. de Bellerive, Lausanne, Switzerland*

18–19 Information Resource Management Symp., NBS, Gaithersburg *S. Torrence, A-640, Administration Bldg., NBS, Wash., D.C. 20234*

22–23 **Optical Fabrication and Testing, OSA Workshop,** N. Falmouth, Mass. *OSA, 1816 Jefferson Pl. N.W., Wash., D.C. 20036*

22–24 National Conference of Standards Laboratories, NBS, Gaithersburg *B. Belanger, B-362 Physics Bldg., NBS, Wash., D.C. 20234*

22–26 Polymers and Fibers course, Chicago *N. Daerr, McCrone Res. Inst., 2508 S. Michigan Ave., Chicago, Ill. 60616*

22–26 COMPCON Fall 80, Wash., D.C. *P.O. Box 639, Silver Spring, Md. 20901*

23–25 Radiation Curing, 5th Int. Conf., Boston *AFP/SME, Soc. of Manufacturing Eng., 1 SME Dr., P.O. Box 930, Dearborn, Mich. 48128*

23–25 European Conf. on Optical Systems and Applications, Utrecht *D. J. Kroon, Philips Res. Labs., Proj. Ctr. Geldrop, W. Alexanderlaan 7B, 5664 AN Geldrop, The Netherlands*

28–30 Photographic Technology Symp., Wash., D.C. *R. Wood, SPSE, 1411 K St., N.W. Suite 930, Wash., D.C. 20005*

28–1 Oct. 2nd Int. Conf. on Lasers in Graphics, San Diego, Calif. *T. Dunn, Dunn Tech., 1131 Beaumont Circle, Vista, CA 92083*

28–3 Oct. FACSS 7th Ann. Mtg., Philadelphia *T. C. Rains, Chem. Bldg., NBS, Washington, D.C. 20234*

29–1 Oct. Ceramics as Archeological Material Conf., NBS, Gaithersburg *A. Franklin, A-355 Materials Bldg., NBS, Wash., D.C. 20234*

29–2 Oct. Applied Superconductivity Conf., Santa Fe, N.M. *W. Keller, LASL, P.O. Box 1663, MS 764, Los Alamos, N.M. 87545*

29–3 Oct. Electrostatics, Electrophotography & Electrostatic Precipitators, Cincinnati *B. Greason, Northern Telecom Canada, P.O. Box 5155, Dept. 2840, London, Ont. N6A 4N3*

29–3 Oct. SPIE Electro-Optical Technical Symp., Huntsville, Ala. *SPIE, P.O. Box 10, Bellingham, Wash. 98225*

30–1 Oct. ASTM Laser Induced Damage in Optical Materials, 12th Ann. Symp., NBS, Boulder *A. Guenther, Air Force Weapons Lab., Kirtland AFB, N.M.*

30–1 Oct. ASTM Optical Materials for High Power Lasers, 12th Ann. Symp., NBS, Boulder *N. Lear, Electromagnetics Div., NBS, 325 W. Broadway, Colo. 80302*

October

6–9 10th Int. Laser Radar Conf., Silver Spring, Md. *T. D. Wilkerson, IPST, U. Md., College Pk., Md. 20742*

6–10 Applied Polarized Light Microscopy course, Chicago *N. Daerr, McCrone Res Inst., 2508 S. Michigan Ave., Chicago, Ill. 60616*

6–10 5th Int. Conf. on Infrared and Millimeter Waves, U. Wurzburg, Germany *K. J. Button, MIT, Cambridge, Mass. 02139*

continued on page 2583